Review

Bin Hu, Ying Zhang and Qi Jie Wang*

Surface magneto plasmons and their applications in the infrared frequencies

Abstract: Due to their promising properties, surface magneto plasmons have attracted great interests in the field of plasmonics recently. Apart from flexible modulation of the plasmonic properties by an external magnetic field, surface magneto plasmons also promise nonreciprocal effect and multi-bands of propagation, which can be applied into the design of integrated plasmonic devices for biosensing and telecommunication applications. In the visible frequencies, because it demands extremely strong magnetic fields for the manipulation of metallic plasmonic materials, nano-devices consisting of metals and magnetic materials based on surface magneto plasmon are difficult to be realized due to the challenges in device fabrication and high losses. In the infrared frequencies, highly-doped semiconductors can replace metals, owning to the lower incident wave frequencies and lower plasma frequencies. The required magnetic field is also low, which makes the tunable devices based on surface magneto plasmons more practically to be realized. Furthermore, a promising 2D material-graphene shows great potential in infrared magnetic plasmonics. In this paper, we review the magneto plasmonics in the infrared frequencies with a focus on device designs and applications. We investigate surface magneto plasmons propagating in different structures, including plane surface structures and slot waveguides. Based on the fundamental investigation and theoretical studies, we illustrate various magneto plasmonic micro/nano devices in the infrared, such as tunable waveguides, filters, and beam-splitters. Novel plasmonic devices such as one-way waveguides and broad-band waveguides are also introduced.

Keywords: plasmonics; surface magneto plasmons; tunable devices; infrared.

DOI 10.1515/nanoph-2014-0026
Received September 28, 2014; accepted January 16, 2015

1 Introduction

Surface Plasmons (SPs) are electromagnetic waves that are confined on and propagate along the interface between a dielectric and a conductor, usually a metal. Because their confining property could break the diffraction limit, SPs are widely applied in the fields from photonic devices, imaging, and data storage to solar cells, and biosensing in recent years, which leads to a new branch of photonics – plasmonics [1–4]. In recent years, in order to realize tunable ultra-miniaturized circuits, many efforts have been made to achieve active plasmonic devices based on thermo-optic, electric-optic and nonlinear optical effects [5–7]. Compared with these tuning mechanisms, which are operated by changing the permittivity of the dielectric, a magnetic field is able to modulate the SPs by changing the permittivity of the conductor.

SPs are caused by the interaction of the incident electromagnetic (EM) waves and the free electrons of the conductor. In the interaction, the free electrons respond collectively by oscillating resonantly with the incident EM waves. The resonant oscillation is characterized by a characteristic frequency – the plasma frequency ω_p, which sets the scale of the free electrons response to time-varying perturbations [8]. Since SPs rely on the motion of the free electrons, it can be imagined that an external magnetic field may influence the SPs properties, due to the Lorentz force altering the response of carriers to frequency perturbations. In this situation, another characteristic frequency called cyclotron frequency ω_c appears, which is

***Corresponding author: Qi Jie Wang,** OPTIMUS, Photonics Centre of Excellence, School of Electrical and Electronic Engineering, Nanyang Technological University, 50 Nanyang Ave., 639798 Singapore; and CDPT, Centre for Disruptive Photonic Technologies, Nanyang Technological University, 637371 Singapore, e-mail: qjwang@ntu.edu.sg
Bin Hu: School of Optoelectronics, Beijing Institute of Technology, Beijing 100081, China
Ying Zhang: Singapore Institute of Manufacturing Technology, 71 Nanyang Drive, 638075 Singapore

Edited by Volker Sorger

proportional to the strength of the applied magnetic field **B** [9]. One of the important consequences of magnetizing the plasmons is that the polarizability becomes highly anisotropic (the permittivity of the conductor ε_c becomes a tensor), which is expressed as

$$\varepsilon_c = \begin{bmatrix} \varepsilon_{xx} & 0 & \varepsilon_{xz} \\ 0 & \varepsilon_{yy} & 0 \\ -\varepsilon_{xz} & 0 & \varepsilon_{xx} \end{bmatrix}, \tag{1}$$

in which

$$\varepsilon_{xx} = \varepsilon_\infty \left[1 - \frac{\omega_p^2(\omega + i\upsilon)}{\omega[(\omega + i\upsilon)^2 - \omega_c^2]} \right], \tag{2}$$

$$\varepsilon_{xz} = -i\varepsilon_\infty \frac{\omega_p^2 \omega_c^2}{\omega[(\omega + i\upsilon)^2 - \omega_c^2]}, \tag{3}$$

$$\varepsilon_{yy} = \varepsilon_\infty \left[1 - \frac{\omega_p^2}{\omega(\omega + i\upsilon)} \right], \tag{4}$$

where ω is the angular frequency of the incident wave, ε_∞ and ε_0 are the high-frequency permittivity and vacuum permittivity, respectively. υ is the collision frequency of free electrons. Therefore, SPs may become very different when they are subject to an external magnetic field, usually called surface magneto plasmons (SMPs) [10].

According to the relationship of the three directions – the orientation of applied magnetic field **B**, the propagation of the surface wave **k**, and the surface, SMPs can be divided in three principal configurations: perpendicular geometry (**B** perpendicular to the surface and **k**), Faraday geometry (**B** parallel to the surface and **k**), and Voigt geometry (**B** parallel to the surface and perpendicular to **k**), as shown in Figure 1. Compared with traditional SPs, SMPs have some unique properties. For example, SMPs in perpendicular and Faraday geometries can support pseudo-surface waves, which attenuate on only one side of the surface, while on the other side, they propagate (SPs attenuate on both sides) [11, 12]. As for Voigt geometry, SMPs in this configuration have two exclusive and intriguing peculiarities. The first one is the two propagating bands. For traditional SPs, they are always supported in one propagating frequency band below the plasma frequency of the conductor [8]. However, when an external magnetic field is applied, a higher SPs band appears above the conductor plasma frequency, and both the higher and lower SPs bands can be tuned by the magnetic field. The second unique property is the nonreciprocal effect. When

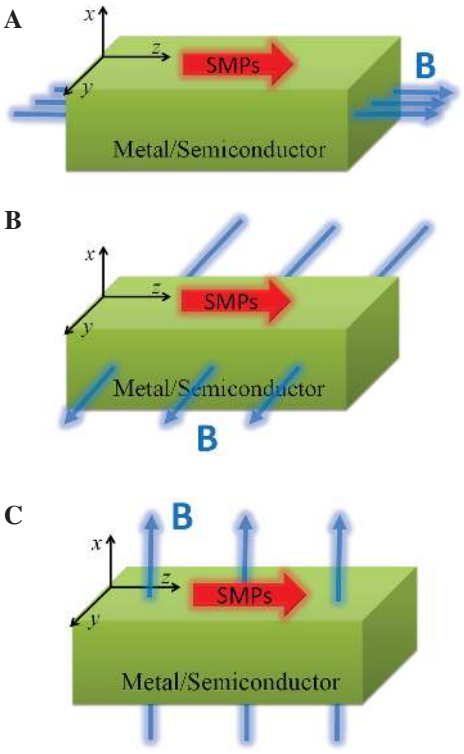

Figure 1: Surface Magneto Plasmons propagating on a conductor surface. (A) Faraday geometry. (B) Voigt geometry. (C) Perpendicular geometry.

the magnetic field is applied in the Voigt configuration, the dispersions of the SMP propagating in two opposite directions are different, which results in that the two SMP waves have various cutoff frequencies.

The researches on SMPs in different structures began many years ago. The basic theories of SMPs on a conductor surface in the perpendicular and Faraday configurations were presented by Brion et al. [11] and Wallis et al. [12] in 1974, respectively. In 1987, Kushwaha gave the theoretical study of SMP modes of a thin film in the Faraday configurations [13]. The pioneer work of SMPs in the Voigt configuration was implemented by Chiu et al. [14] and Brion et al. [15] as early as 1972, separately. Then in the same year, De Wames and coworkers studied the dispersion relation of SMPs in the Voigt configuration of a thin film [16]. In the following years, many theoretical works about SMP properties were proposed considering the holes [17], optical phonons [18–20], diffuse electron density profiles [21], and metal screen [22]. They were also studied both theoretically and experimentally in various structures [23–34]. In 2001, Kushwaha gave a review of SMP researches until then [35].

In recent years, due to the extraordinary optical transmission through periodic holds in nanometer scale, which is found in 1998 [36], numerous plasmonic devices, made of metals, have been theoretically proposed and experimentally realized in the visible frequencies. Compared with traditional studies on SPs before 2000 [37–46], these structures were mostly focused on subwavelength confinement and manipulation of electromagnetic waves [3]. For example, in the slot waveguide structure [47] (also called the metal-insulator-metal structure [48]), light can be confined in the lateral dimension as small as ~0.1 λ. Based on these works, some SMP devices, which are also consisted of metals, were proposed [49–54]. However, all of these SMP structures are hard to realize in laboratories because the required magnetic field is too strong to realize. According to Eq. (1–4), in order to observe the effect of the external magnetic field, it requires that ω_p, ω_c and the incident angular frequency ω should be comparable. However, for a metal in the visible frequencies, ω_p and ω are usually in the order of ~10^{16} and ~10^{15} Hz, respectively. Therefore, it needs a magnetic field as strong as ~10^3 Tesla, although the largest achievable magnetic field in the laboratory is ~10^2 Tesla. So far, there are two main ways to solve this problem. The first one is using composite materials, including metals and ferromagnetic materials, such as Ni and Co [55–62]. Using this method, due to the strong magnetization of the ferromagnetic materials, the applied magnetic field can be as weak as several ~mT. Recently, a review article is presented for the SMPs in composite magnetic materials [63]. However, it introduces large loss and the nonreciprocal effect and the two propagating bands are rarely observed. Another solution is decreasing both ω_p and ω_c, i.e., using semiconductors instead of metals. Through doping in a semiconductor, ω_p can be as low as ~10^{13} Hz. In consequence, the required external magnetic field is <2 Tesla. However, this is only valid in the infrared (IR) regime.

In this article, we will focus on recent works about IR SMPs, especially the Voigt geometry, using semiconductors in some structures, i.e., periodic grating and subwavelength slot waveguides, and their applications in SMP devices design. In Section 2, we will give the propagation of IR SMPs on a semiconductor surface. In Section 3, we will introduce SMPs propagating in subwavelength slot waveguides (semiconductor-insulator-semiconductor (SIS) structure) and its applications. Some intriguing plasmonic devices based on these structures will be presented, including one-way waveguides and broadly tunable THz slow light waveguides. In Section 4, a new semiconductor material-graphene applied in IR SMPs is introduced. In Section 5, we will give the conclusion.

2 Surface magneto plasmons on a semiconductor surface

SMPs propagating on a semiconductor plane surface was first investigated. The first theory of SMPs on a semiconductor plane surface in the Voigt configuration was presented by Chiu et al. [14]. From the Maxwell equations, they gave the dispersion relation of the SMPs as

$$\varepsilon_d\sqrt{\beta^2-k_0^2\varepsilon_V}+\varepsilon_V\sqrt{\beta^2-k_0^2\varepsilon_d}+i\beta\varepsilon_d\frac{\varepsilon_{xz}}{\varepsilon_{xx}}=0, \tag{5}$$

where β is the wave vector of SMPs, k_0 is the wave vector in vacuum, ε_d is the permittivity of the dielectric, c is the light velocity in vacuum. $\varepsilon_V=\varepsilon_{xx}+\varepsilon_{xz}^2/\varepsilon_{xx}$ is the Voigt dielectric constant, which can be considered as the bulk dielectric constant. It can be clearly seen from Eq. (5) that this dispersion is nonreciprocal with respect to the direction of propagation, i.e., the positive and negative values of the wave vector β are not equivalent. The numerical solution of Eq. (5) for *n*-doped InSb was given by Brion et al. in the same year. They found both the nonreciprocal effect and the two propagating bands as shown in Figure 2A.

As shown in the dispersion equation, the nonreciprocal effect and two propagating bands is immediately observed. For $\beta>0$, the lower curve starts from the origin, and terminates when it reaches the dispersion curve of the bulk magneto plasmons (the line marked as $\alpha=sqrt(\beta-\varepsilon_V\omega^2/c^2)=0$). The higher branch starts from the line of $\varepsilon_{xx}=0$, and approaches the asymptotic frequency for the non-retarded magneto plasmons defined by $\varepsilon_d+\varepsilon_{xx}-i\varepsilon_{xz}=0$. However, for $\beta<0$, the lower band starting from the origin to the asymptotic value defined by $\varepsilon_d+\varepsilon_{xx}+i\varepsilon_{xz}=0$. The higher band starts at the light line $\varepsilon_{xx}=1$, and cutoff when it meets the higher bulk magneto plasmon curve $\alpha=0$. They also gave an explanation of why the higher band appears. As shown in Figure 2B, there are two regions corresponding with $\varepsilon_V<0$ when $\omega_c=0.5\,\omega_p$. Because SMPs can only propagate on the surface of a material with negative permittivity, SMPs have two propagating bands on a plane surface.

Although the novel effect of SMPs on a plane surface was discovered several decades ago, plasmonic IR devices based on SMPs were only proposed in recent years after the boom of plasmonics. In 2010, Lan et al. developed a long-range SMPs waveguide consists of an InSb film with the Voigt geometry [64]. The nonreciprocal effects, similar to that of SMPs on a plane surface, can be found in the waveguide, as shown in Figure 3. When the magnetic field is not applied, the mode profile is symmetric with the film. However, when the magnetic field B is applied, the field distribution becomes asymmetric, and changes when the magnetic field applied in the opposite direction.

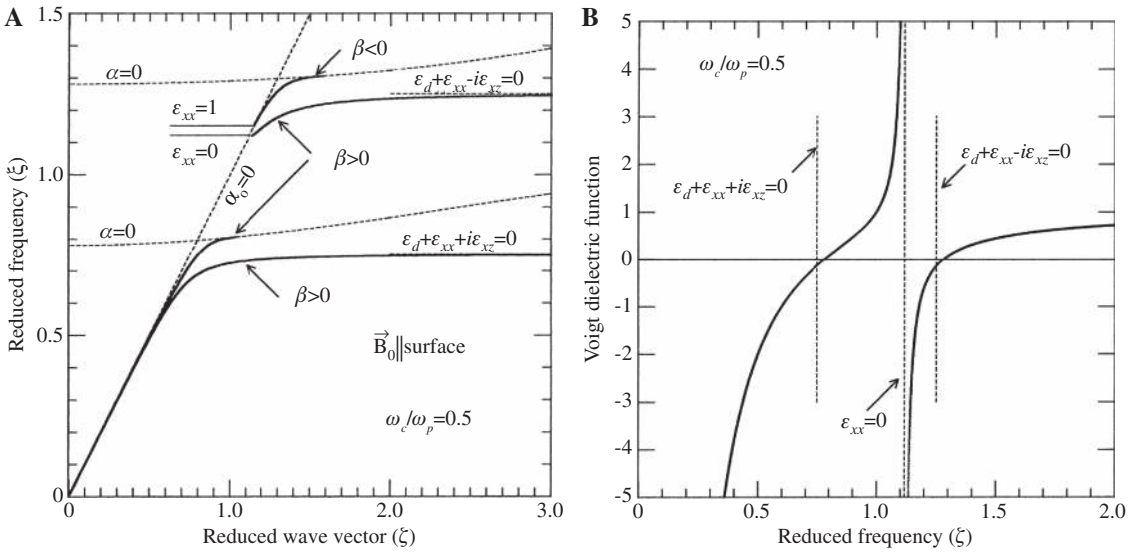

Figure 2: (A) Dispersion curves of SMPs at the interface of *n*-type InSb and air in the Voigt configuration (solid lines). (B) Voigt dielectric constant ε_v as a function of frequency (Reprinted from Surf Sci Report, 41, Kushwaha MS, Plasmons and magnetoplasmons in semiconductor heterostructures, 1–416, Copyright (2001), with permission from Elsevier.).

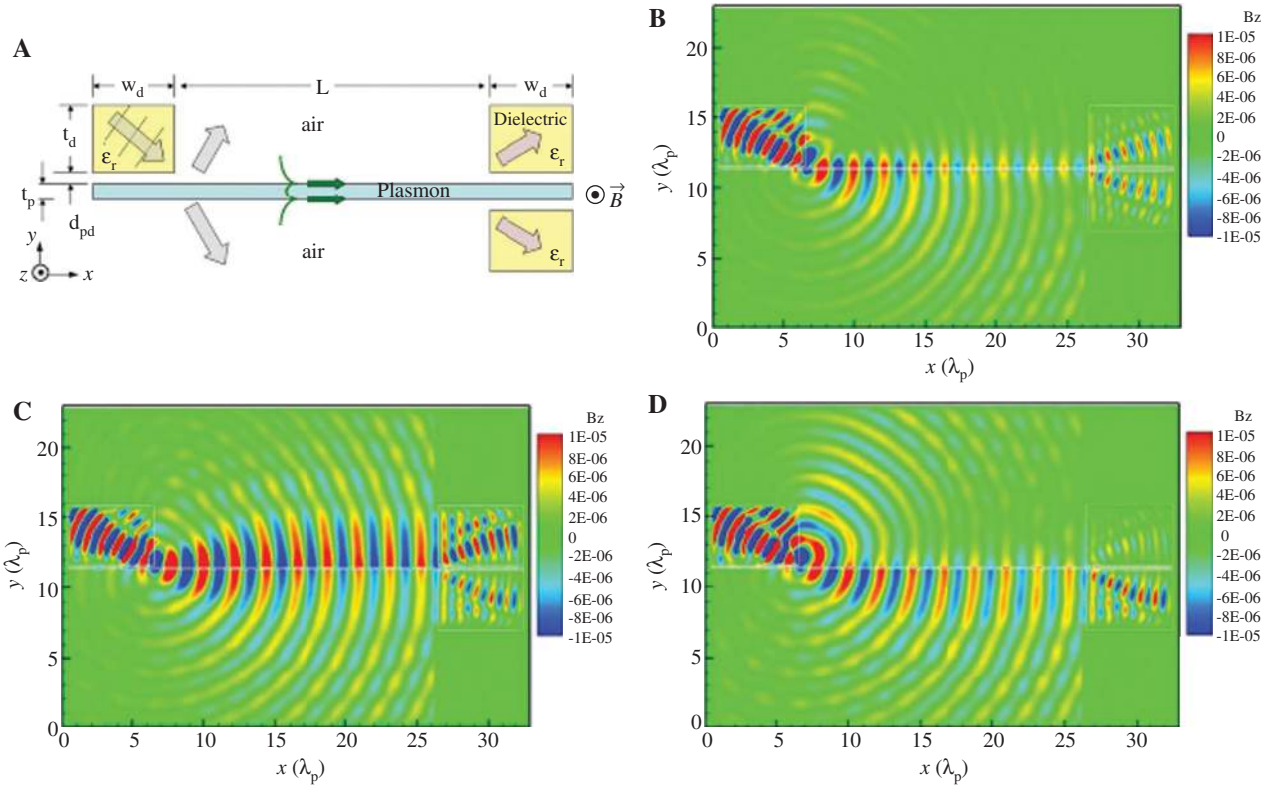

Figure 3: SMPs dispersion on a semiconductor thin film, with ω_c=0.5 ω_p (from [64]). (A) Schematic structure of the long-range SMPs waveguide. Field distribution of film SMPs mode when B=0 (B), B in the -y direction (C) and B in the +y direction (D), with ω=0.45 ω_p, ω_c=1.0 ω_p, d=0.15×2$\pi c/\omega_p$.

The propagating form of SMPs is not strict to plane SPs. They can also propagate in other forms, e.g., Airy wave packets. Airy SPs can propagate on a metal surface with intriguing properties of non-diffracting, asymmetric field profile, self-bending, and self-healing. It is first proposed theoretically by Salandrino and Christodoulides [65], and

realized experimentally by different ways [66, 67]. In 2012, Hu et al. proposed analytically that Airy SMPs are supported on semiconductor planes [68]. Furthermore, the external magnetic field can manipulate the self-deflection property of the Airy SMPs by tuning the wave vector of SMPs, as shown in Figure 4. They found that when a magnetic field is applied, the ballistic trajectory of the Airy SMPs can be tuned depending on the direction of the applied magnetic field due to the nonreciprocal effect.

3 Surface magneto plasmons in slot waveguides and their applications

In order to tune the SPs confinement, plasmonic slot waveguide consisting of an insulator with subwavelength thickness sandwiched by two metal slabs are proposed and studied for achieving high confinement. This structure is also widely applied for SMPs. The slot waveguides for SMPs can be divided into two structures: symmetric (the two semiconductor slabs are same) and asymmetric structures (the two semiconductor slabs are different), as shown in Figure 5A and B. The SMPs dispersion of these two structures are expressed by

$$\tanh\left(w\sqrt{\beta^2-\varepsilon_d k_0^2}\right)\left[1+\left(\frac{\varepsilon_d}{\varepsilon_V}\right)^2\frac{\beta^2-\varepsilon_V k_0^2}{\beta^2-\varepsilon_d k_0^2}+\left(\frac{\varepsilon_d}{\varepsilon_V}\right)^2\left(\frac{\varepsilon_{xz}}{\varepsilon_{xx}}\right)^2\frac{\beta^2}{\beta^2-\varepsilon_d k_0^2}\right]+2\frac{\varepsilon_d}{\varepsilon_V}\frac{\sqrt{\beta^2-\varepsilon_V k_0^2}}{\sqrt{\beta^2-\varepsilon_d k_0^2}}=0, \tag{6a}$$

$$\left\{\frac{\sqrt{\beta^2-k_0^2\varepsilon_m}\sqrt{\beta^2-k_0^2\varepsilon_V}}{\beta^2-\varepsilon_d k_0^2}\frac{1}{\varepsilon_m\varepsilon_V}+\frac{1}{\varepsilon_d^2}-i\frac{\beta\sqrt{\beta^2-k_0^2\varepsilon_m}}{\beta^2-\varepsilon_d k_0^2}\frac{\varepsilon_{xz}}{\varepsilon_m\varepsilon_V\varepsilon_{xx}}\right\}\tanh\left(\sqrt{\beta^2-\varepsilon_d k_0^2}w\right)+\left[\frac{\sqrt{\beta^2-k_0^2\varepsilon_V}}{\sqrt{\beta^2-\varepsilon_d k_0^2}}\frac{1}{\varepsilon_d\varepsilon_V}+\frac{\sqrt{\beta^2-k_0^2\varepsilon_m}}{\sqrt{\beta^2-\varepsilon_d k_0^2}}\frac{1}{\varepsilon_m\varepsilon_d}-i\frac{\beta}{\sqrt{\beta^2-\varepsilon_d k_0^2}}\frac{\varepsilon_{xz}}{\varepsilon_d\varepsilon_V\varepsilon_{xx}}\right]=0 \tag{6b}$$

respectively, where ε_m is the insulator permittivity, ε_m and ε_V are the dielectric constants of the two semiconductor slabs, respectively. An intriguing feature of Eq. (6) is that the nonreciprocal effect is only found in the asymmetric structure. The dispersion relations of these two structure are plotted in Figure 5C and D. It can be found that although the dispersion curve is reciprocal in the symmetric

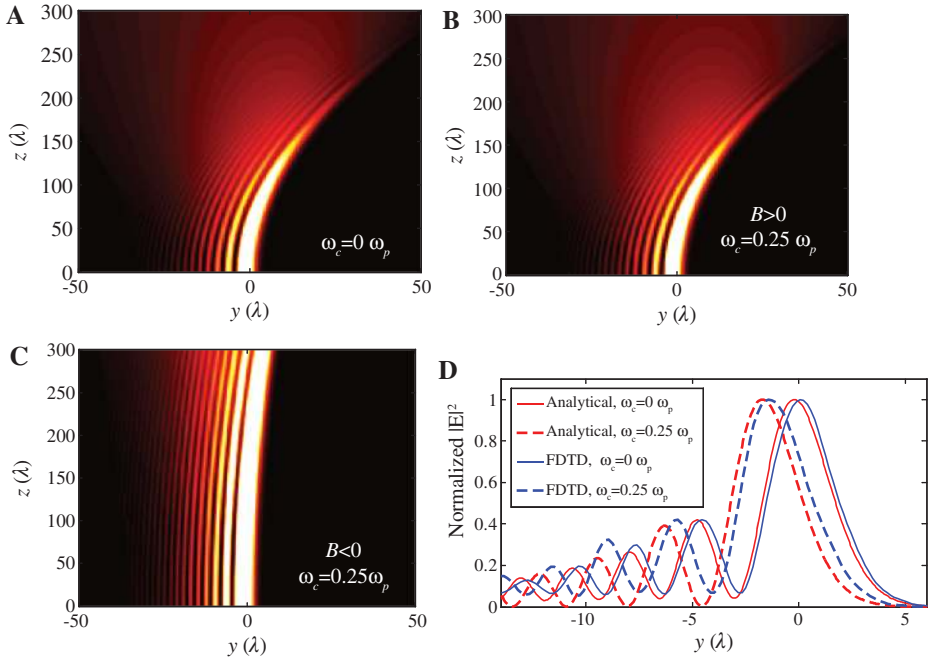

Figure 4: Magnetic field tuning of Airy SMPs (from [68]). Theoretical calculated electric fields of the Airy SMPs on the semiconductor surface with an incident frequency of ω=0.85 ω when (A) No magnetic field is applied, (B) A magnetic field is applied with ω_c=0.25 ω_p, and (C) A magnetic field is applied with ω_c=0.25 ω_p. (D) Comparison of theory (red lines) and FDTD simulation (blue lines) results of normalized electric field distributions after Airy SMPs propagate 50 λ. Solid lines: field distributions when ω_c=0 ω_p. Dashed lines: field distributions when ω_c=0.25 ω_p for B<0.

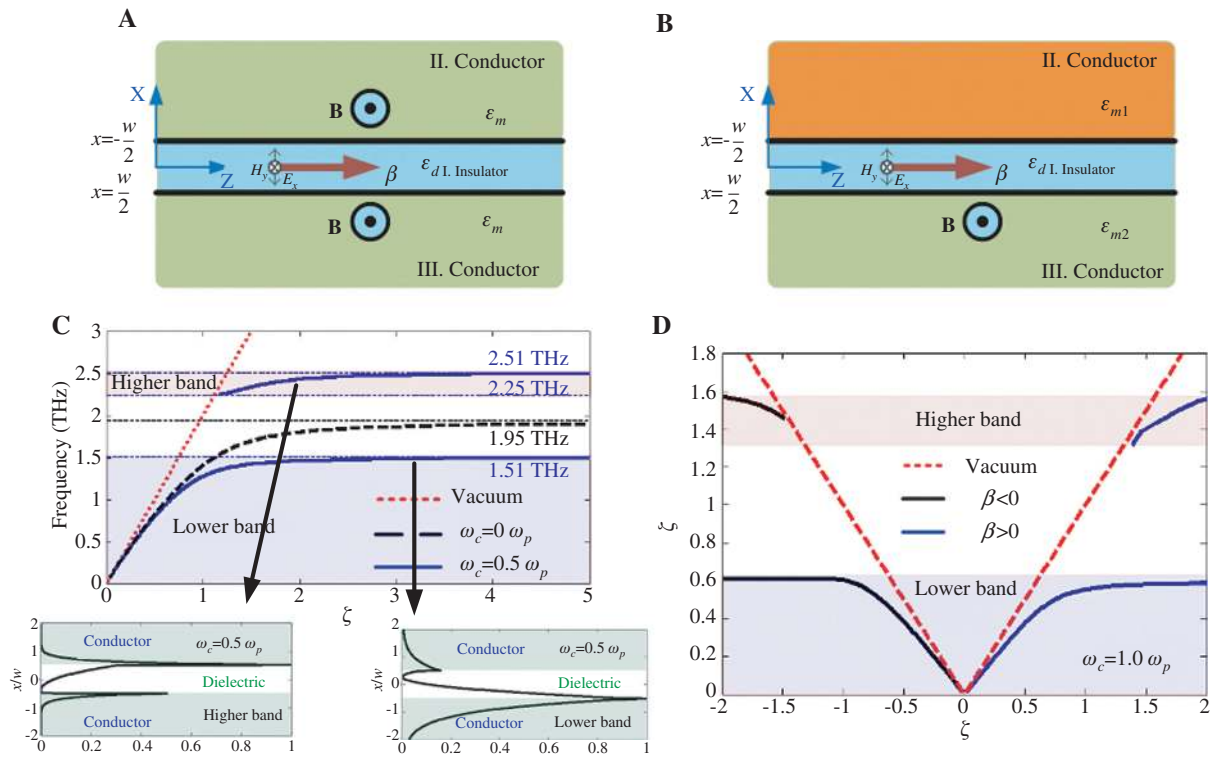

Figure 5: SMPs propagating in a slot waveguide. (A) Schematic of the symmetric structure. (B) Schematic of the asymmetric structure. (C) SMPs dispersion of the symmetric structure with (ω_c=0.5 ω_p) and without (ω_c=0 ω_p) the magnetic field. The insets shows the electric field distribution in the slot waveguide for the higher and lower bands, respectively. (D) SMPs dispersion of the asymmetric structure with (ω_c=ω_p) the magnetic field.

structure, the lower and higher mode distributions are not the same, which is shown in the inset of Figure 5C. For the asymmetric structure, the nonreciprocal effect is reflected by that the forward propagating and backward propagating SMPs have different cutoff frequencies.

Several kinds of plasmonic IR devices based on the slot SMPs have been proposed in recent years. The symmetric structure are often used for design of magnetic-field tunable devices. For example, periodically arranged slot waveguides can be used as tunable filters. At first, this kind of filters were made of semiconductor gratings with subwavelength slits [69–73]. By changing the external magnetic fields, the propagation of SMPs in the slits is modulated, which leads to the shift of the transmission peak, as shown in Figure 6A and B. In 2013, a terahertz (THz) wave filter consists of Bragg grating structure is proposed [71]. Both magnetic field tuning and high Q-value was able to be realized (Figure 6C).

Another kind of tunable devices are phase modulators. A tunable planar plasmonic slit lens (PSL) was proposed in 2011 [74]. PSLs are often used to realize integrated optical collimators, consisting of a metallic slab, perforated with several well-designed nano-slits with various widths, thicknesses or material compositions. When a light wave propagates through these slits, it has different phase retardations. Therefore, focus of light can be realized by adjusting the materials and geometric parameters of the slits through the phase control. Compared to other plasmonic lenses, PSLs have relatively simple structures, which can be easily fabricated. In addition, it has a better design flexibility because traditional diffraction optics theory, e.g., some iteration algorithms, can be applied to obtain the desired slit parameters. By replacing the metal with semiconductor, a tunable THz lens was well designed. With the intensity of the external magnetic field increased to 1 Tesla, the focal length was tuned by 3 λ, which is shown in Figure 7.

Compared with SPs, which have only one propagating band, SMPs have two bands, providing a possibility of realizing broad band devices. For example, a broad band IR slow light waveguide. Slow-light technology introduces a wealth of applications in telecommunications, data processing, and light-matter interactions recently. Compared with traditional electronic approaches, Plasmonic approaches are easy to achieve on-chip devices due to its subwavelength confinement of electromagnetic (EM)

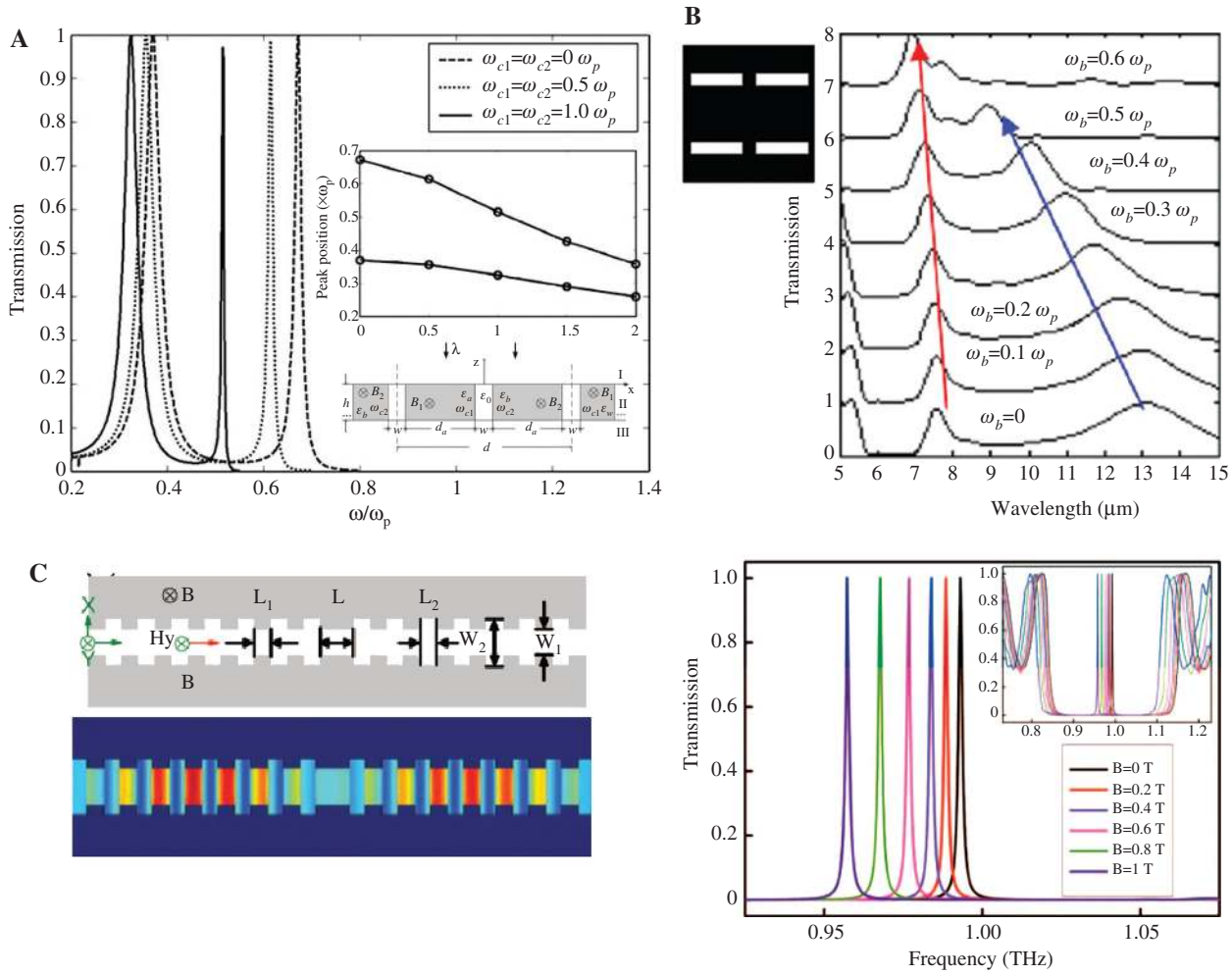

Figure 6: SMPs filters based on 1D grating (A) (from [69]), 2D grating (B) (Reprinted from Solid State Commun, 149, Zhou R, Li H, Zhou B, Wu L, Liu X, Gao Y, Transmission through a perforated metal film by applying an external magnetic field, 657–661, Copyright (2009), with permission from Elsevier), and Bragg grating (C) (Li K, Ma X, Zhang Z, Wang L, Hu H, Xu Y, Song G., Highly tunable Terahertz filter with magneto-optical Bragg grating formed in semiconductor-insulator-semiconductor waveguides, AIP Advances, Vol. 3, (2013); used in accordance with the Creative Commons Attribution 3.0 Unported License). All these filters can be tuned by the external magnetic field.

fields. However, most slow light systems are not tunable so far, especially in the IR frequency region. Hu et al. presented a magnetic-field tunable THz slow-light system based on SMPs in a semiconductor-insulator-semiconductor (SIS) structure [75]. In this system, the group velocity of the slowed-down THz wave can be tuned by the external magnetic field (Figure 8). More importantly, due to the existence of two SMPs bands, especially the higher band, the proposed system has a very broad tunable bandwidth. They showed that when the external magnetic field increases from 0 to 6 Tesla, a monochromatic THz wave in a range of [0.3, 10] THz can be slowed down in a lossless InSb-air-InSb structure. Interestingly, with the increase of the magnetic fields, the velocity of the THz wave deceases for the lower band, while that of the THz wave increase for the higher band.

Because the SMPs in asymmetric slot structure have the nonreciprocal effect, this structure is usually applied in one-way EM wave systems. In a One-way-propagating waveguide, light waves can only propagate in the forward or the backward directions, thus it is of particular importance for isolators, switches and splitters. One method to realize one-way plasmonic devices are based on interference of SPs [76]. This effect is strongly sensitive to geometric structure variations. Another approach is by the nonreciprocal effect of SMPs under an external magnetic field. The dispersions of the forward and backward propagating SMPs terminate at different cut-off frequencies, making it possible to realize an absolute one-way plasmonic waveguide. One IR one-way sub-wavelength plasmonic waveguide was reported in 2012 [77]. The waveguide is composed of an Au-dielectric-InSb structure as

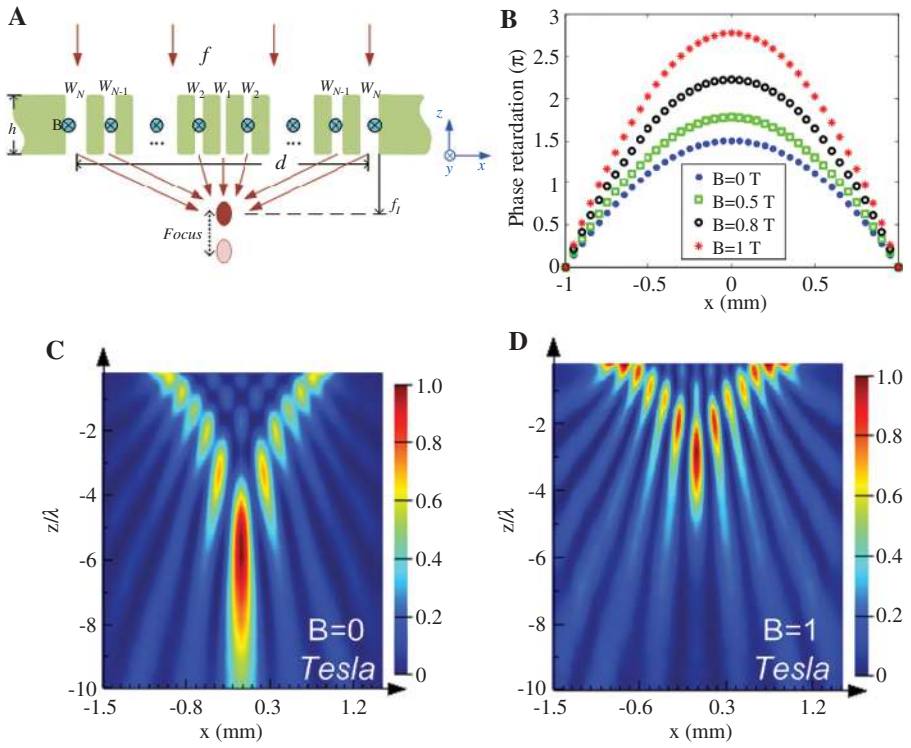

Figure 7: A tunable plasmonic lens (from [74]). (A) Schematic structure of the lens. The structure consists of an InSb slab tunable by an external magnetic field *B*, and perforated with 2*N*-1 sub-wavelength slits. (B) The relative phase retardation of the slits under magnetic fields of 0, 0.5, 0.8 and 1 Tesla. (C), (D) Field distributions of the structure when the external magnetic field is 0 Tesla and 1 Tesla, respectively.

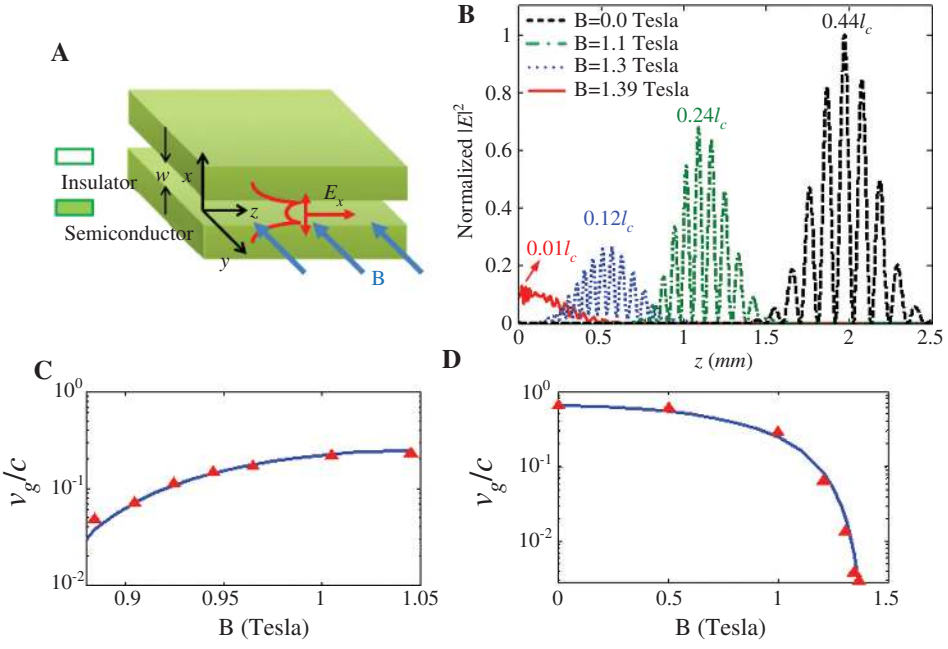

Figure 8: A terahertz (THz) tunable slow-light system. (A) Schematic structure of the slow-light system (from [75]). (B) FDTD simulations of THz pulses propagating in the slow-light waveguide. The frequency of the incident wave is 1 THz. When the magnetic fields are 0, 1.1, 1.3, and 1.4 Tesla, the peak of the pulse moves $0.01l_c$, $0.12l_c$, $0.24l_c$, and $0.44l_c$ after the THz pulse is launched 15*ps*, respectively, where l_c is defined as l_c=15*ps*×*c*. (C) and (D) (from [75]): Group velocity of a monochromatic wave tuning by the magnetic field. *f*=1 THz (in the lower band) and *f*=3 THz (in the higher band), respectively.

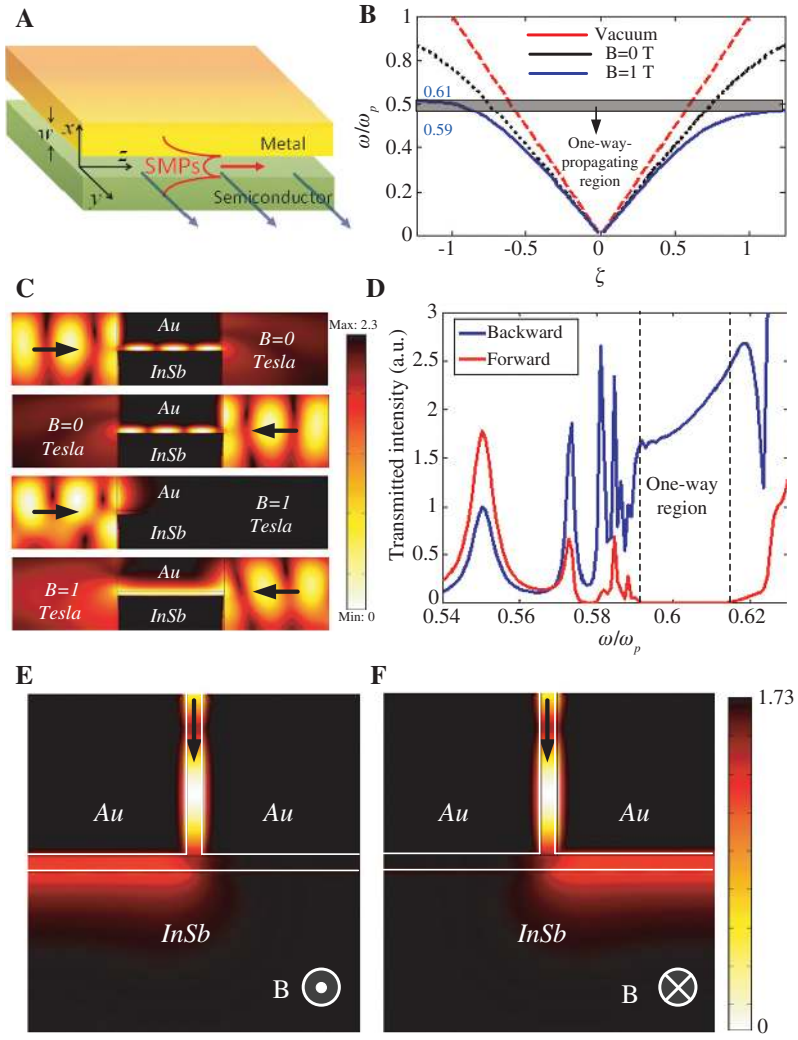

Figure 9: A one-way infrared (IR) waveguide based on the nonreciprocal effect of SMPs (from [77]). (A) Schematic structure of the one-way THz plasmonic waveguide. It is composed of metal (upper), dielectric (middle), and semiconductor (lower) layers. (B) Dispersion relations of the THz SMPs without and with an external magnetic field. (C) FEM-simulated field distribution of the forward and backward propagating waves in a sub-wavelength slit. The width and length of the slit are $0.1\times 2\pi c/\omega_p$ and 300 μm, respectively. The incident frequency is ω=0.6 ω_p, which is in the one-way frequency band. (D) Transmitted intensities of the forward and backward propagating waves when 1 Tesla magnetic field is applied. (E) and (F): Field distributions of a designed THz plasmonic switch when the magnetic field is along +*y*-axis and along -*y*-axis, respectively.

depicted in Figure 9(A). From the dispersion curves of the lower band of SMPs (Figure 9B), it can be seen that without the magnetic field, the dispersion curves are symmetric. While, when magnetic field is applied, the dispersion curves of the two propagating waves are different. The forward-propagating mode vanishes at a frequency of ω/ω_p=0.59, while the backward propagating mode vanishes at a higher frequency of ω/ω_p=0.61. This means that the THz waves in the frequency region of ω/ω_p=[0.59, 0.61] (corresponding to f=[1.18, 1.23] THz) can only propagate backwards. The simulations verified the one-way effect (Figure 9C and D). By this one-way waveguide, a T-shape plasmonic switch was designed, depending on the direction of the applied magnetic field (Figure 9C and D).

Based on the one-way waveguide, some other one-way devices were proposed. Fan et al. designed a THz isolator consisting of a metallic slab and periodic semiconductor pillars [78]. The operating frequency of the isolator can be broadly tuned from 1.4 to 0.9 THz by changing the external magnetic field from 0.6 to 1.6 Tesla at 195 K. They also proposed a nonreciprocal PSL based on the asymmetric slot waveguide [79], by which the focus can be only found for the forward propagating IR waves, as shown in Figure 10. This device combines the properties of lenses

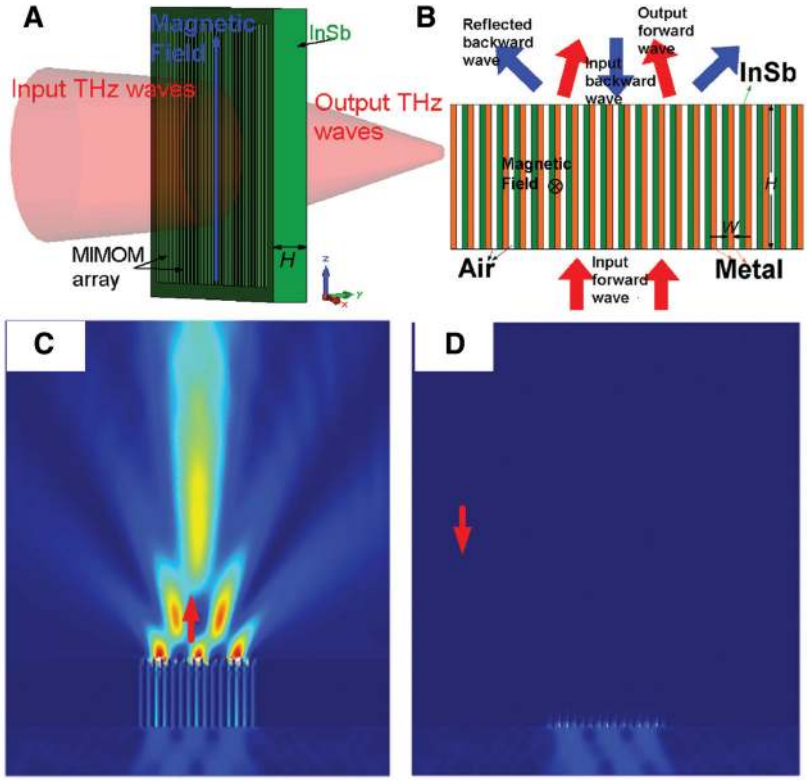

Figure 10: A one-way plasmonic slit lens (PSL) (from [79]). (A) and (B): Schematic structure of the lens. It consists of many asymmetric slot waveguide units. Each unit is composed of metal, air and InSb. (C) and (D): Forward and backward power flow distributions through the PSL.

and filters, which could be applied in THz imaging and communications.

4 Surface magneto plasmons on a 2D material-graphene

Although plasmonic devices based on SMPs can be realized by semiconductors, most magnetic field-tunable devices are designed for THz frequencies, because only in this regime, the plasma frequency, the cyclotron frequency and incident frequency are comparable for most semiconductors, thus the effect of the SMPs can be observed. Are we able to design SMPs devices in the mid-IR frequencies? This problem would be solved by a new material – graphene. Graphene is a rapidly rising star on the horizon of materials science, condensed-matter physics, electronics and photonics [80, 81]. It is a flat monolayer of carbon atoms tightly packed into a two-dimensional (2D) honeycomb lattice (Figure 11A), which had been presumed not to exist in the free state [82], until it was first produced by micromechanical exfoliation of graphite in 2004 [83, 84]. The 2D honeycomb lattice of graphene leads to a rather unique band structure. In the absence of doping, conduction and valence bands of graphene touch at six so-called Dirac points (Figure 11B) [85, 86], which is also the position of the Fermi energy. For low energies, the dispersion around the Dirac point is linear, in which the graphene charge carriers are indeed massless Dirac fermions. Hence graphene has many unusual physical properties, such as a "minimum" conductivity of ~$4e^2/h$ even when the carrier concentration tends to zero [80]. Another intriguing property of graphene band structure is that it can be controlled by the chemical potential (μ, also Fermi level E_F) through chemical doping or electrical gating (Figure 11C).

The unique structure also gives graphene attractive photonic properties, including the outstanding carrier mobility, the good trans-conductance, and the ultimate thinness and stability [85], which enables graphene a good photonic material. In plasmonics, it has been proved that graphene has appealing properties including extreme confinement, tunability, crystallinity, and supporting both TM and TE modes [87]. Besides the unique properties, similar to the metal SPPs, the propagation of graphene SPPs is also able to be engineered by surface structures.

In the presence of a magnetic field perpendicular to a 2D graphene sheet, the resonances originating from the

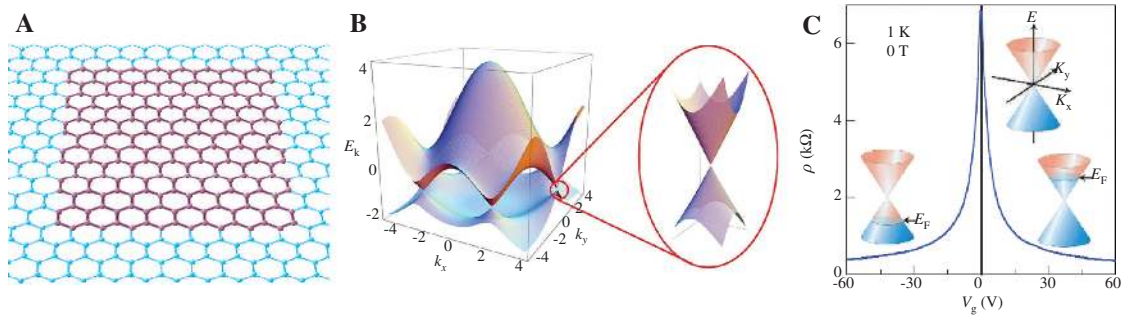

Figure 11: (A) Hexagonal honenycomb lattice of graphene (Reprinted by permission from Macmillan Publishers Ltd: Nat. Mater [80], copyright (2007)). (B) Electronic band structure of graphene. Right: zoom in of the energy bands close to one of the Dirac points (from [81], http://dx.doi.org/10.1103/RevModPhys.81.109). (C) Electric field effect on resistivity in single-layer graphene. The insets show its conical low-energy spectrum E(k), indicating changes in the position of the Fermi energy E_F with changing gate voltage V_g (from [80]).

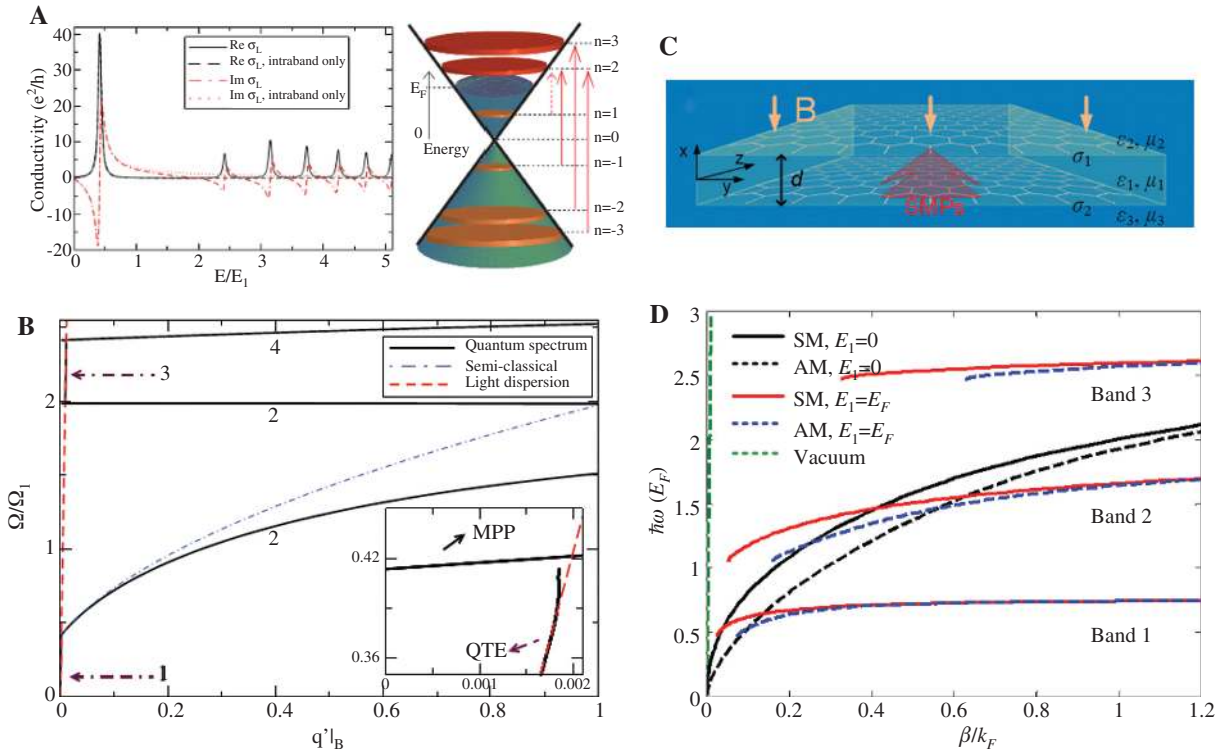

Figure 12: (A) Conductivity of doped graphene in a magnetic field (from [90], http://dx.doi.org/10.1103/PhysRevB.85.205426). (B) Dispersion relation of SMPs on a single layer graphene (from [90]). (C) Schematic structure of SMPs propagating on a double layer graphene (from [91]). (D) Dispersion relation of SMPs on a double layer graphene (from [91]).

cyclotron effect in the classical regime and the inter-Landau-level transitions in the quantum regime could lead to a strong Faraday rotation, which can be used for fast tunable ultrathin magneto-optical devices [88, 89]. Furthermore, the massless free carriers in graphene result in non-equidistant Landau levels (LLs) and specific electron-electron excitations (Figure 12A). These non-equidistant Landau levels make that the dispersion curve of the SMP mode splits into a series of branches. The dispersion of the SMP propagating on a single layer graphene was first given by Ferreira et al. [90]. They found that that graphene supports not only SMP modes, but also a sequence of weakly decaying modes called quasi-transverse-electric modes, which correspond to the TE mode without the magnetic fields (Figure 12B). In addition all these modes are tunable by changing the magnetic field or the Fermi energy. SMPs propagating in the structure of double layer graphene are then studied by Hu et al. [91]. Compared with the structure

of single layer graphene, SMPs in double layer graphene have two modes: symmetric and antisymmetric modes (Figure 12C and D). Although the magnetic field has little effect on the coupling of the symmetric and antisymmetric modes, the decoupling of these two modes can be achieved by varying the doping levels of the two graphene layers.

5 Conclusions

In this paper, we give a brief review on SMPs in the IR frequencies. Because of the lower incident frequency and cyclotron frequency, SMP devices are mostly made of semiconductors. First, the SMPs on a plane semiconductor surface, in symmetric and asymmetric slot waveguide are reviewed. We also give the applications of SMPs based on their unique and intriguing properties, such as the nonreciprocal effect, two propagating bands, and tunability by an external magnetic field, which show SMPs have great opportunities in applications of tunable plasmonic devices. Although the development of SMPs still has some challenges, including large losses and requiring strong magnetic fields, with the rapid development of plasmonic research SMPs may open a new avenue for manipulating lights in subwavelength range in the IR range.

Acknowledgments: This work is supported by the Ministry of Education, Singapore (MOE2011-T2-2-147 and MOE2011-T3-1-005), and the CNRS International – NTU-Thales Research Alliance (CINTRA) Laboratory, UMI 3288, Singapore 637553. The support from NCET, China, and Project-sponsored by SRF for ROCS, SEM, China (To Dr. Bin Hu), as well as the National Basic Research Program of China (973 Program Grant Nos. 2013CBA01702 and 2013CB328801) are also acknowledged.

References

[1] Barnes WL, Dereux A, Ebbesen TW. Surface plasmon subwavelength optics. Nature 2003;424:824–30.
[2] Ozbay E. Plasmonics: merging photonics and electronics at nanoscale dimensions. Science (New York, NY) 2006;311:189–93.
[3] Ebbesen TW, Genet C, Bozhevolnyi SI. Surface-plasmon circuitry. Phys Today 2008;61:44–50.
[4] Gramotnev DK, Bozhevolnyi SI. Plasmonics beyond the diffraction limit. Nat. Photonics 2010;4:83–91.
[5] Nikolajsen T, Leosson K, Bozhevolnyi SI. Surface plasmon polariton based modulators and switches operating at telecom wavelengths. Appl Phys Lett 2004;85:5833–5.
[6] Dicken MJ, Sweatlock LA, Pacifici D, Lezec HJ, Bhattacharya K, Atwater HA. Electrooptic modulation in thin film barium titanate plasmonic interferometers. Nano Letters 2008;8:4048–52.
[7] Min C, Wang P, Jiao X, Deng Y, Ming H. Beam manipulating by metallic nano-optic lens containing nonlinear media. Opt Express 2007;15:9541–6.
[8] Raether H. Surface plasmons on smooth and rough surfaces and on gratings. In: Chapter 2.1: Fundamental Properties: Dispersion Relation, Extension and Propagation Length for the Electromagnetic Fields of the Surface Plasmons. Hohler G., ed. Springer, Berlin, 1988.
[9] Palik ED, Furdyna JK. Infrared and microwave magnetoplasma effects in semiconductors. Rep Prog Phys 1970;33:1193–322.
[10] Brion JJ, Wallis RF, Hartstein A, Burstein E. Theory of surface magnetoplasmons in semiconductors. Phys Rev Lett 1972;28:1455–8.
[11] Brion JJ, Wallis RF. Theory of pseudosurface polaritons in semiconductors in magnetic fields. Phys Rev B 1974;10:3140–3.
[12] Wallis RF, Brion JJ, Burstein E. Theory of surface polaritons in anisotropic dielectric media with application to surface magnetoplasmons in semiconductors. Phys Rev B 1974;9:3424–37.
[13] Kushwaha MS, Halevi P. Magnetoplasma modes in thin films in the faraday configuration. Phys Rev B 1987;35:3879–89.
[14] Chiu KW, Quinn JJ. Magnetoplasma surface waves in metals. Phys Rev B 1972;5:4707–9.
[15] Brion JJ, Wallis RF, Hartstein A, Burstein E. Theory of surface magnetoplasmons in semiconductors. Phys Rev Lett 1972;28:1455–8.
[16] De Wames RE, Hall WF. Magnetic field effect on plasma-wave dispersion in a dielectric layer. Phys Rev Lett 1972;29:172–5.
[17] Flahive PG, Quinn JJ. Surface waves of an electron-hole plasma in a uniform magnetic field. Phys Rev Lett 1973;31:586–9.
[18] Brion JJ, Wallis RF, Hartstein A, Burstein E. Interaction of surface magnetoplasmons and surface optical phonons in polar semiconductors. Surf Sci 1973;34:73–80.
[19] Hartstein A, Burstein E, Palik ED, Gammon RW, Henvis BW. Investigation of optic-phonon – magnetoplasmon-type surface polaritons on n-InSb. Phys Rev B 1975;12:3186.
[20] Palik ED, Kaplan R, Gammon RW, Kaplan H, Wallis RF, Quinn JJ. Coupled surface magnetoplasmon-optic-phonon polariton modes on InSb. Phys Rev B 1976;13:2497.
[21] Eguiluz A, Quinn JJ. Magnetoplasma surface waves in solids with diffuse electron density profiles. Phys Rev B 1976;13:4299–305.
[22] Yi KS, Quinn JJ. Magnetoplasma surface waves of a degenerate semiconductor in the faraday geometry: effect of the presence of a metallic screen. Phys Rev B 1980;22:6247–53.
[23] Tyler IL, Fischer B, Bell RJ. On the observation of surface magnetoplasmons. Opt Commun 1973;8:145–6.
[24] Kaplan H, Palik ED, Kaplan R, Gammont RW. Calculation of attenuated-total-reflection spectra of surface magnetoplasmons on semiconductors. J Opt Soc Am A 1974;64:1551–62.
[25] Fisher AD. Optical guided-wave interactions with magnetostatic waves at microwave frequencies. Appl Phys Lett 1982;41:779.
[26] Remer L, Mohler E, Grill W, Lüthi B. Nonreciprocity in the optical reflection of magnetoplasmas. Phys Rev B 1984;30:3277.
[27] Stamps RL, Camley RE. Focusing of magnetoplasmon polaritons. Phys Rev B 1985;31:4924.
[28] Camley RE. Nonreciprocal surface waves. Surf Sci Report 1987;7:103–87.

[29] Kushwaha M, Halevi P. Magnetoplasmons in thin films in the Voigt configuration. Phys Rev B 1987;36:5960–7.
[30] Glass N. Nonreciprocal diffraction via grating coupling to surface magnetoplasmons. Phys Rev B 1990;41:7615.
[31] Boardman A, Shabat M, Wallis R. Nonlinear surface magnetoplasmon waves on a semiconductor. Opt commun 1991;86:416–22.
[32] Elmzughi F, Tilley D. Surface and guided-wave polariton modes of magnetoplasma films in the Voigt geometry. J Phys: Condensed Matt 1994;6:4233.
[33] Safarov V, Kosobukin VA, Hermann C, Lampel G, Peretti J, Marlière C. Magneto-optical effects enhanced by surface plasmons in metallic multilayer films. Phys Rev Lett 1994;73:3584–7.
[34] Hermann C, Kosobukin VA, Lampel G, Peretti J, Safarov VI, Bertrand P. Surface-enhanced magneto-optics in metallic multilayer films. Phys Rev B 2001;64:235422.
[35] Kushwaha MS. Plasmons and magnetoplasmons in semiconductor heterostructures. Surf Sci Report 2001;41:1–416.
[36] Ebbesen T, Lezec HJ, Ghaemi HF, Thio1 T, Wolff PA. Extraordinary optical transmission through sub-wavelength hole arrays. Nature 1998;391:667–9.
[37] Ritchie RH, Arakawa ET, Cowan JJ, Hamm RN. Surface-plasmon resonance effect in grating diffraction. Phys Rev Lett 1968; 21:1530–3.
[38] Economou E. Surface plasmons in thin films. Phys Rev 1969;182:539–54.
[39] Marschall N, Fischer B, Queisser H. Dispersion of surface plasmons in InSb. Phys Rev Lett 1971; 27:95–7.
[40] Knop K. Rigorous diffraction theory for transmission phase gratings with deep rectangular grooves. J Opt Soc America 1978;68:1206.
[41] Moreland J, Adams A, Hansma PK. Efficiency of light emission from surface plasmons. Phys Rev B 1982;25:2297–300.
[42] Sheng P, Stepleman R, Sanda P. Exact eigenfunctions for square-wave gratings: application to diffraction and surface-plasmon calculations. Phys Rev B 1982;26:2907–16.
[43] Weber M, Mills D. Interaction of electromagnetic waves with periodic gratings: enhanced fields and the reflectivity. Phys Rev B 1983;27:2698–709.
[44] Sambles J, Bradbery G, Yang F. Optical excitation of surface plasmons: an introduction. Contemp Phys 1991;32:173–83.
[45] Yang F, Sambles J, Bradberry G. Long-range surface modes supported by thin films. Phys Rev B 1991;44:5855–72.
[46] Lochbihler H. Surface polaritons on gold-wire gratings. Phys Rev B 1994;50:4795–801.
[47] Dionne J, Sweatlock LA, Atwater HA, Polman A. Plasmon slot waveguides: Towards chip-scale propagation with subwavelength-scale localization. Phys Rev B 2006;73:035407.
[48] Kurokawa Y, Miyazaki H. Metal-insulator-metal plasmon nanocavities: Analysis of optical properties. Phys Rev B 2007;75:035411.
[49] Belotelov V, Doskolovich L, Zvezdin A. Extraordinary magneto-optical effects and transmission through metal-dielectric plasmonic systems. Phys Rev Lett 2007;98:077401.
[50] Johnson BL, Shiau HH. Guided magneto-plasmon polaritons in thin films: non-reciprocal propagation and forbidden modes. J Phys: Condensed Matt 2008;20:335217.
[51] Yu Z, Veronis G, Wang Z, Fan S. One-way electromagnetic waveguide formed at the interface between a plasmonic metal under a static magnetic field and a photonic crystal. Phys Rev Lett 2008;100:23902.
[52] Hadad Y, Steinberg B. Magnetized spiral chains of plasmonic ellipsoids for one-way optical waveguides. Phys Rev Lett 2010;105:233904.
[53] Lan YC, Chang YC, Lee PH. Manipulation of tunneling frequencies using magnetic fields for resonant tunneling effects of surface plasmons. Appl Phys Lett 2007;90:171114.
[54] Khanikaev A, Mousavi SH, Shvets G, Kivshar YS. One-way extraordinary optical transmission and nonreciprocal spoof plasmons. Phys Rev Lett 2010;105:126804.
[55] Ferreiro-Vila E, González-Díaz JB, Fermento R, González MU, García-Martín A, García-Martín JM, Cebollada A, Armelles G, Meneses-Rodríguez D, Sandoval EM. Intertwined magneto-optical and plasmonic effects in Ag/Co/Ag layered structures. Phys Rev B 2009;80:125132.
[56] Drezdzon SM, Yoshie T. On-chip waveguide isolator based on bismuth iron garnet operating via nonreciprocal single-mode cutoff. Opt Express 2009;17:9276–81.
[57] Temnov V, Armelles G, Woggon U, Guzatov D, Cebollada A, Garcia-Martin A, Garcia-Martin J-M, Thomay T, Leitenstorfer A, Bratschitsch R. Active magneto-plasmonics in hybrid metal-ferromagnet structures. Nat Photon 2010;4:107–11.
[58] Torrado JF, González-Díaz JB, González MU, García-Martín A, Armelles G. Magneto-optical effects in interacting localized and propagating surface plasmon modes. Opt Express 2010;18:15635–42.
[59] Zhu H, Jiang C. Nfonreciprocal extraordinary optical transmission through subwavelength slits in metallic film. Opt Lett 2011;36:1308–10.
[60] Belotelov VI, Akimov IA, Pohl M, Kotov VA, Kasture S, Vengurlekar AS, Gopal AV, Yakovlev DR, Zvezdin AK, Bayer M. Enhanced magneto-optical effects in magnetoplasmonic crystals. Nat Nanotechnol 2011;6:370–6.
[61] Ferreiro-Vila E, Iglesias M, Paz E, Palomares FJ, Cebollada F, González JM, Armelles G, García-Martín JM, Cebollada A. Magneto-optical and magnetoplasmonic properties of epitaxial and polycrystalline Au/Fe/Au trilayers. Phys Rev B 2011;83:205120.
[62] Bonanni V, Bonetti S, Pakizeh T, Pirzadeh Z, Chen J, Nogués J, Vavassori P, Hillenbrand R, Ākerman J, Dmitriev A. Designer magnetoplasmonics with nickel nanoferromagnets. Nano letters 2011;11:5333–8.
[63] Armelles G, Cebollada A, García-Martín A, González MU. Magnetoplasmonics: combining magnetic and plasmonic functionalities. Adv Opt Mater 2013;1:10.
[64] Lan YC, Chen CM. Long-range surface magnetoplasmon on thin plasmon films in the Voigt configuration. Opt Express 2010;18:12470.
[65] Salandrino A, Christodoulides DN. Airy plasmon: a nondiffracting surface wave. Opt Lett 2010;35:2082.
[66] Minovich A, Klein AE, Janunts N, Pertsch T, Neshev DN, Kivshar YS. Generation and near-field imaging of Airy surface plasmons. Phys Rev Lett 2011;107:116802.
[67] Li L, Li T, Wang SM, Zhang C, Zhu SN. Plasmonic Airy beam generated by in-plane diffraction. Phys Rev Lett 2011;107:126804.
[68] Hu B, Wang QJ, Zhang Y. Voigt Airy surface magneto plasmons. Opt Express 2012;20:21187.
[69] Hu B, Gu B, Dong B, Zhang Y. Optical transmission resonances tuned by external static magnetic field in an n-doped semiconductor grating with subwavelength slits. Opt Commun 2008;281:6120.

[70] Zhou R, Li H, Zhou B, Wu L, Liu X, Gao Y. Transmission through a perforated metal film by applying an external magnetic field. Solid State Commun 2009;149:657–61.
[71] Li K, Ma X, Zhang Z, Wang L, Hu H, Xu Y, Song G. Highly tunable Terahertz filter with magneto-optical Bragg grating formed in semiconductor-insulator-semiconductor waveguides. AIP Advances 2013;3:062130.
[72] Liu XX, Tsai CF, Chern RL, Tsai DP. Dispersion mechanism of surface magnetoplasmons in periodic layered structures. Appl Opt 2009;48:3102–7.
[73] Liu Z, Jin G. Extraordinary THz transmission through sub-wavelength semiconductor slits under antiparallel external magnetic fields. Appl Phys A 2011;105:819–25.
[74] Hu B, Wang QJ, Kok SW, Zhang Y. Active focal length control of terahertz slitted plane lenses by magnetoplasmons. Plasmonics 2011;7:191.
[75] Hu B, Wang QJ, Zhang Y. Slowing down terahertz waves with tunable group velocities in a broad frequency range by surface magneto plasmons. Opt Express 2012;20:10071–6.
[76] Chen J, Li Z, Yue S, Gong Q. Efficient unidirectional generation of surface plasmon polaritons with asymmetric single-nanoslit. Appl Phys Lett 2010;97:041113.
[77] Hu B, Wang QJ, Zhang Y. Broadly tunable one-way terahertz plasmonic waveguide based on nonreciprocal surface magneto plasmons. Opt Lett 2012;37:1895.
[78] Fan F, Chang SJ, Gu WH, Wang XH, Chen AQ. Magnetically tunable terahertz isolator based on structured semiconductor magneto plasmonics. IEEE Photon Technol Lett 2012;24:2080.
[79] Fan F, Chen S, Wang XH, Chang SJ. Tunable nonreciprocal terahertz transmission and enhancement based on metal/magneto-optic plasmonic lens. Opt Express 2013;21:8614–21.
[80] Geim AK, Novoselov KS. The rise of graphene. Nat Mater 2007;6:183–91.
[81] Castro Neto A, Guinea F, Peres N, Novoselov K, Geim A. The electronic properties of graphene. Rev Modern Phys 2009;81:109–62.
[82] Fradkin E. Critical behavior of disordered degenerate semiconductors. Phys Rev B 1986;33:3263–8.
[83] Novoselov KS, Geim AK, Morozov SV, Jiang D, Zhang Y, Dubonos SV, Grigorieva IV, Firsov AA. Electric field effect in atomically thin carbon films. Science 2004;306:666–9.
[84] Novoselov KS, Jiang D, Schedin F, Booth TJ, Khotkevich VV, Morozov SV, Geim AK. Two-dimensional atomic crystals. Proc Natl Acad Sci USA 2005;102:10451–3.
[85] Avouris P. Graphene: electronic and photonic properties and devices. Nano Lett 2010;10:4285–94.
[86] Jablan M, Buljan H, Soljačić M. Plasmonics in graphene at infrared frequencies. Phys Rev B 2009;80:245435.
[87] Christensen J, Manjavacas A, Thongrattanasiri S, Koppens FHL, de Abajo FJG. Graphene plasmon waveguiding and hybridization in individual and paired nanoribbons. ACS nano 2012;6:431–40.
[88] Crassee I, Levallois J, Walter AL, Ostler M, Bostwick A, Rotenberg E, Seyller T, van der Marel D, Kuzmenko AB. Giant Faraday rotation in single- and multilayer graphene. Nat Phys 2010;7:48–51.
[89] Crassee I, Orlita M, Potemski M, Walter AL, Ostler M, Seyller Th, Gaponenko I, Chen J, Kuzmenko AB. Intrinsic terahertz plasmons and magnetoplasmons in large scale monolayer graphen. Nano Lett 2012;12:2470–4.
[90] Ferreira A, Peres N, Castro Neto A. Confined magneto-optical waves in graphene. Phys Rev B 2012;85:205426.
[91] Hu B, Tao J, Zhang Y, Wang QJ. Magneto-plasmonics in graphene-dielectric sandwich. Opt Express 2014;22:21727.